Support Information

Preparation of Cyclodextrin Polymer-Functionalized Polyaniline/ MXene Composites for High-Performance Supercapacitor

Tingting He[1], Xusen Li[1], Bingxin Sun[1], Liwei Lin[2, 3], Fang Guo[4] *, Guowang Diao[1], Yuanzhe Piao[3, 5], Wang Zhang[1, 3,6] *

[1] School of Chemistry and Chemical Engineering, Yangzhou University, Yangzhou, Jiangsu, 225009, P.R. China

[2] School of Petrochemical Engineering, Changzhou University, Changzhou, Jiangsu, 213164, P.R. China

[3] Department of Applied Bioengineering, Graduate School of Convergence Science and Technology, Seoul National University, Seoul, 08826, Republic of Korea

[4] School of Chemistry and Chemical Engineering, Yancheng Institute of Technology, Yancheng, Jiangsu, 224051, P. R. China

[5] Advanced Institutes of Convergence Technology, 145 Gwanggyo-ro, Yeongtong-gu, Suwon-si, Gyeonggi-do, 16229, Republic of Korea

[6] Research Institute for Convergence Science, Seoul National University, Seoul, 08826, Republic of Korea

*Corresponding author: zhangwang@yzu.edu.cn, zhangwang@snu.ac.kr (W. Z.); gfycit@163.com (F. G.)

Electrochemical tests were performed on an electrochemical workstation (CH Instruments, 760E). In three-electrode systems, 1 mol·L^{-1} H_2SO_4 solution was used as electrolyte, a saturated calomel electrode (SCE) served as reference electrode and a platinum wire worked as counter electrode. The working electrode was glassy carbon electrode (GCE) modified with 5×10^{-6} L of composite dispersion at a concentration of 1 mg·mL^{-1} and the GCE needs to be polished with alumina before use. EIS Nyquist plots of the modified electrodes were acquired in 0.1 mol·L^{-1} KCl solution containing a 5 mmol·L^{-1} $[Fe(CN)_6]^{3-/4-}$ mixture (1:1). For two-electrode systems, composite, acetylene black and polyvinylidene fluoride were mixed in an 8:1:1 mass ratio for slurry. The prepared slurry was coated onto a titanium foil as the working electrodes of symmetric supercapacitors. The mass of active material on each electrode was 1.0~1.4 mg. 1 mol·L^{-1} H_2SO_4 solution was used as the electrolyte and filter papers were utilized as the separator. The CV curves at varying scanning rates and the GCD curves at varying current densities were obtained in the voltage window ranging from 0 to 1.0 V. The mass capacitance (C, F·g^{-1}) of the electrode was determined from the GCD curves as expressed by the following equation:

$$C = \frac{I\Delta t}{m\Delta V}$$

where I denotes the current (A), Δt is the constant current discharge time (s), m is the mass of the active substance (g), and ΔV is the applied potential range (V).

Kinetic analysis was performed to explore the charge-storage mechanism of the CDP-PANI/HCS electrode in a 1 M H_2SO_4 solution. The contributions of the three processes to the electrode were calculated: the non-faradaic contribution from the double-layer capacitance, the faradaic contribution from the redox reaction with surface atoms, and the diffusion-controlled redox reaction for the faradaic contribution. For the CV curves, the capacitive effect can be evaluated using the b value determined from the following equation:

$$i = av^b$$

where i denotes the current (A), v is the potential sweep rate (V s^{-1}), and a and b are adjustable parameters. In particular, the value of b was close to 0.5, indicating that the reaction process was dominated by ion diffusion. When the value of b was close to 1.0, surface-controlled pseudocapacitive behavior was observed.

Mathematical analysis of the contributions of the capacitive and diffusion-controlled processes was performed as expressed by the following equations:

$$i(V) = k_1 v + k_2 v^{1/2}$$

$$i(v)/v^{1/2} = k_1 v^{1/2} + k_2,$$

where $k_1 v$ and $k_2 v^{1/2}$ denote the capacitance and diffusion contributions, respectively.

The energy density and power density of the SC was calculated using the following equation:

$$E_S = \frac{1}{2} C_S \Delta V^2$$

$$P_S = E_S / \Delta t$$

where ΔV is the voltage window. Where Ed is the energy density and t is the discharge time.

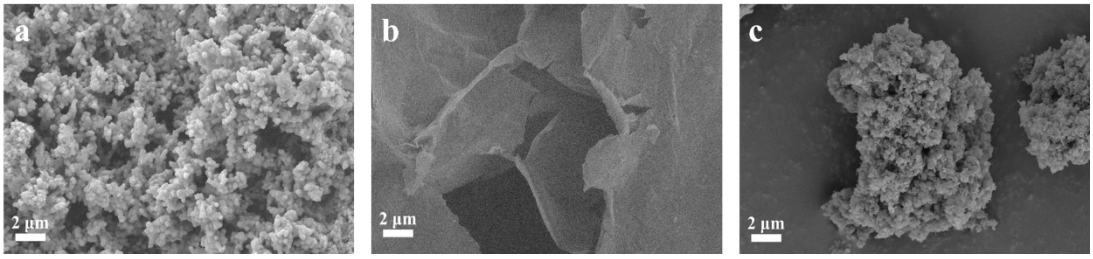

Fig. S1. SEM of (a) PANi; (b) MXene; (c) MX/PA-80.

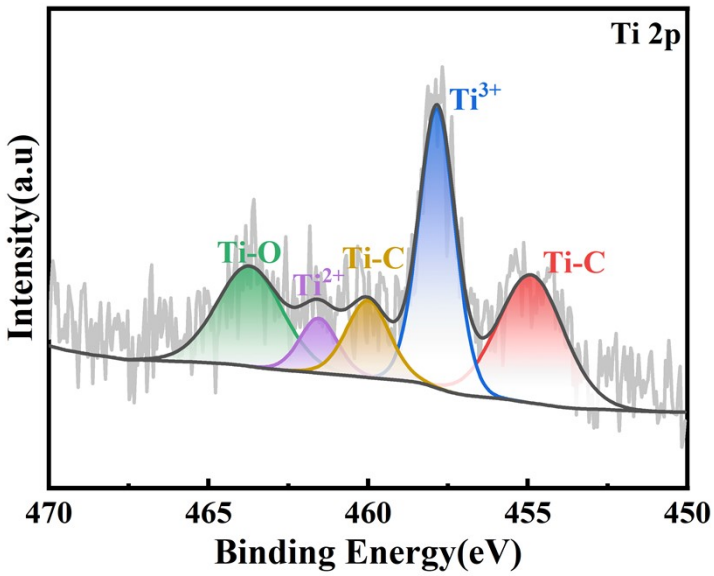

Fig. S2. Ti 2p spectrum of CDP-MX/PA-80

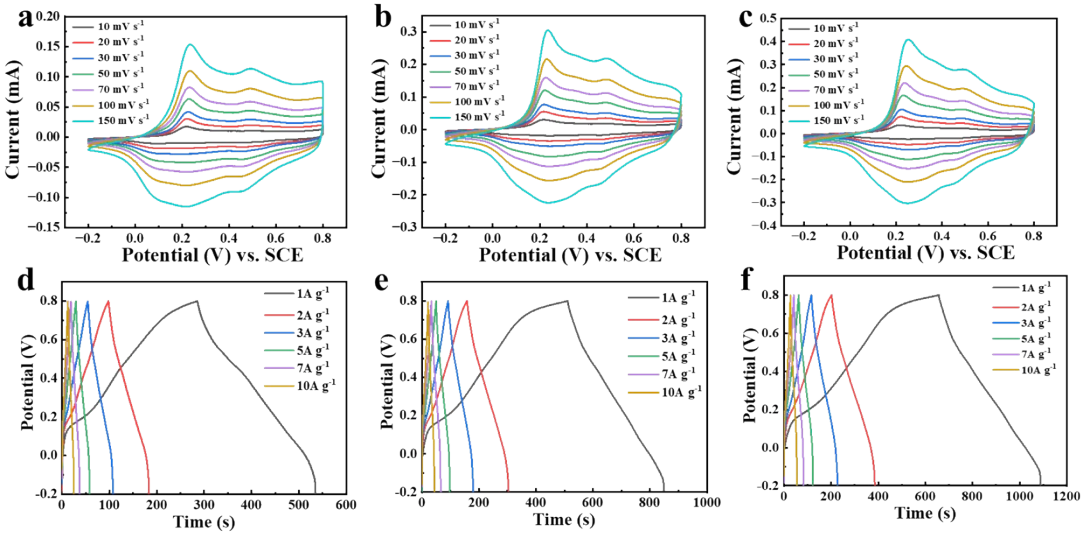

Fig. S3. CV of (a) CDP-MX/PA-40; (b) CDP-MX/PA-60; (c) CDP-MX/PA-100 at scanning speeds of 10-150 mV s^{-1}; GCD of (d) CDP-MX/PA-40; (e) CDP-MX/PA-60; (f) CDP-MX/PA-100 at current densities of 1-10 A g^{-1}.

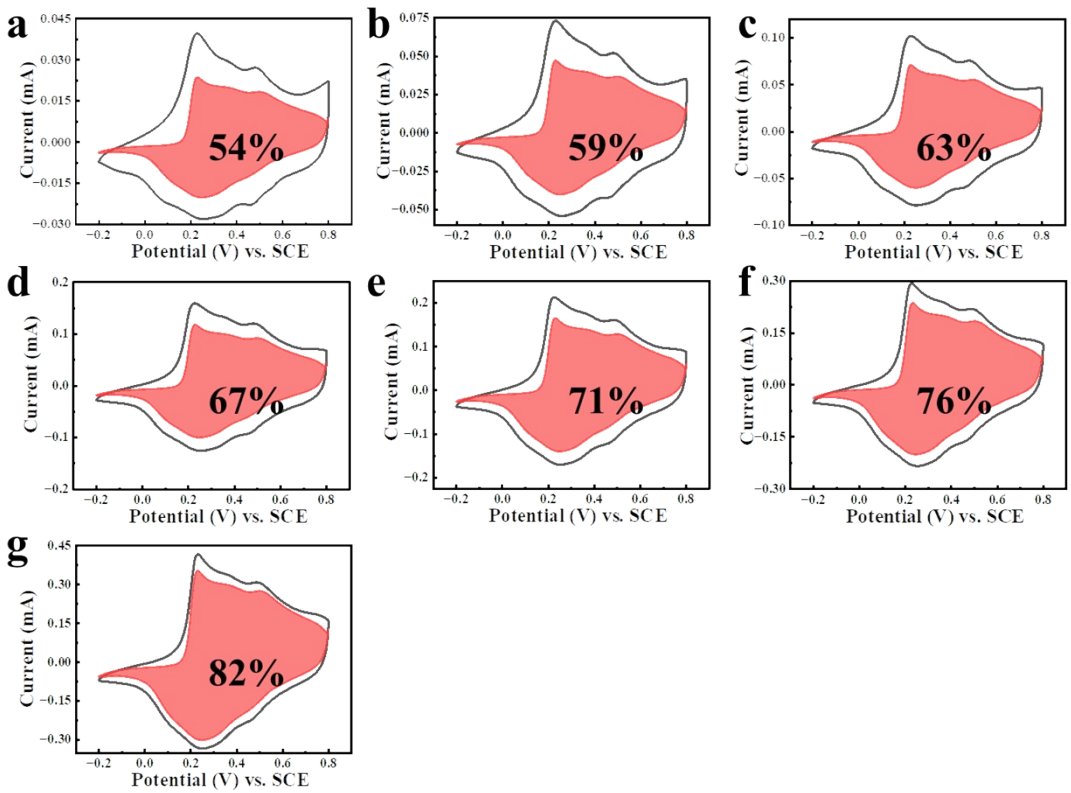

Fig. S4. CV curves of CDP-MX/PA-80 with separation between total current (black line) and capacitive currents (red line) at (a) 10; (b) 20; (c) 30; (d) 50; (d) 70; (d) 100 and (e) 150 mV s^{-1} in 1 M H_2SO_4.

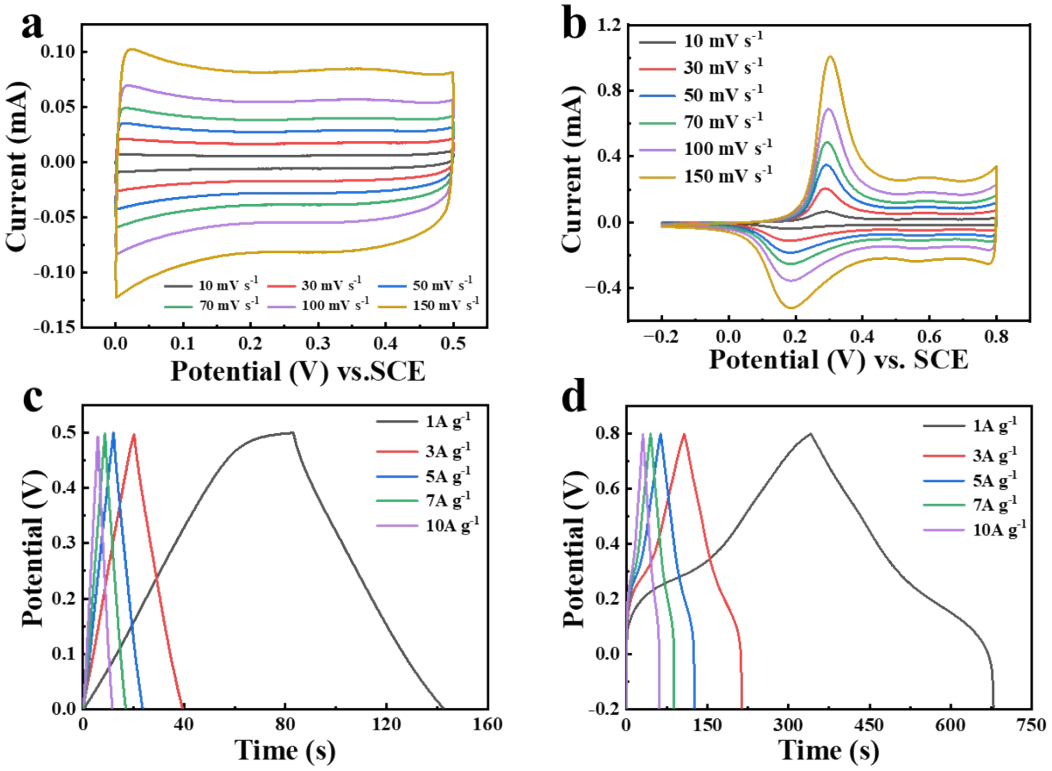

Fig. S5. CV of (a) MXene; (b) PANi at scanning speeds of 10-150 mV s^{-1}. GCD of (c) MXene; (d) PANi at current densities of 1-10 A g^{-1}.

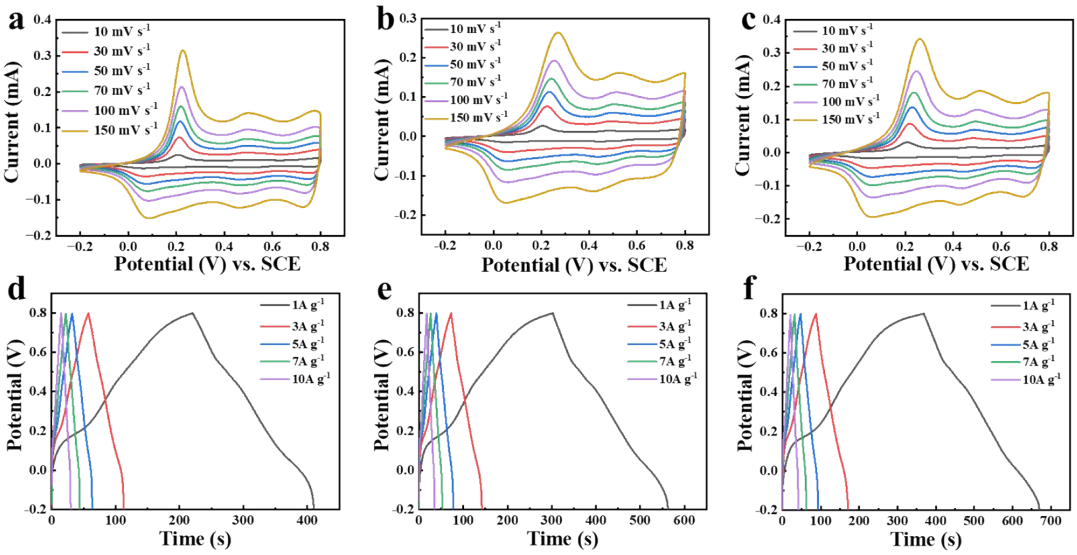

Fig. S6. CV of (a) MX/PA-20; (b) MX/PA-40; (c) MX/PA-60 at scanning speeds of 10-150 mV s^{-1}. GCD of (d) MX/PA -20; (e) MX/PA -40; (f) MX/PA -60 at current densities of 1-10 A g^{-1}.

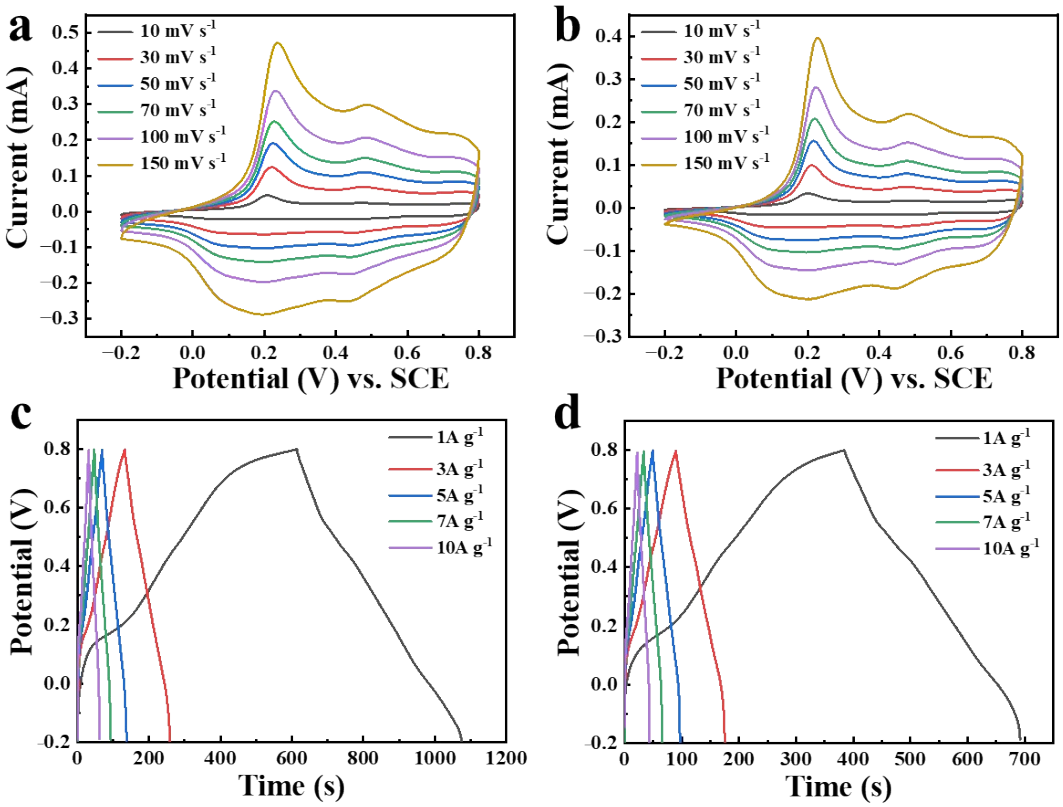

Fig. S7. CV of (a) MX/PA-80, (b) MX/PA-100 at scanning speeds of 10-150 mV s^{-1}; GCD of (c) MX/PA -80, (d) MX/PA -100 at current densities of 1-10 A g^{-1}.

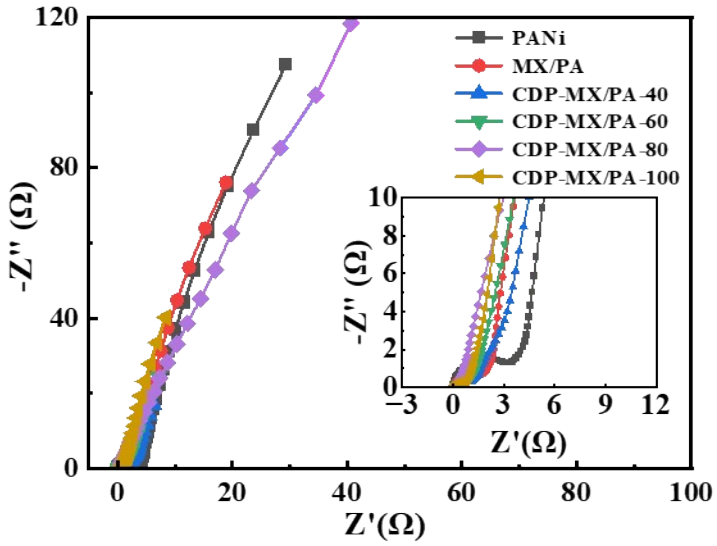

Fig. S8. Nyquist plots of PANI; MX/PA; CDP-MX/PA-40; CDP-MX/PA-60; CDP-MX/PA-80; CDP-MX/PA-100.

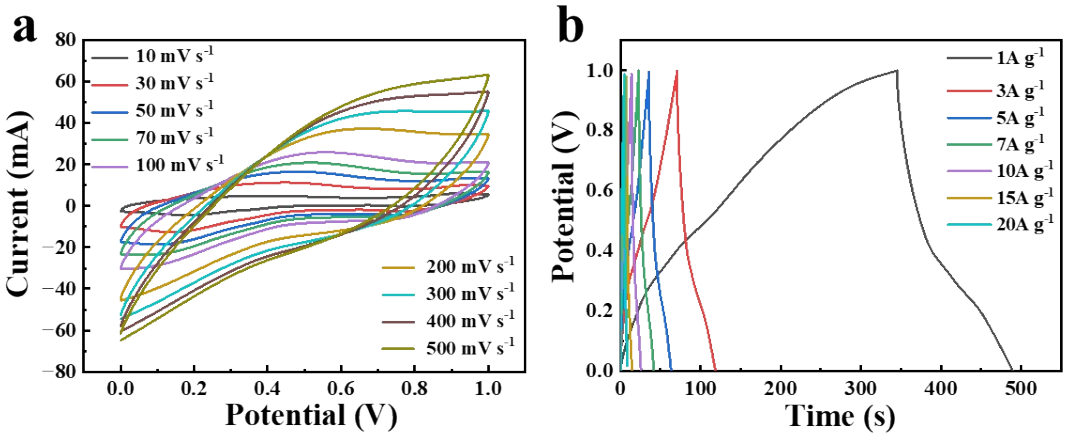

Fig. S9. (a) CV curves of MX/PA||MX/PA supercapacitor at different scan rates, respectively; (c) GCD curves of MX/PA||MX/PA supercapacitor at different current densities, respectively.

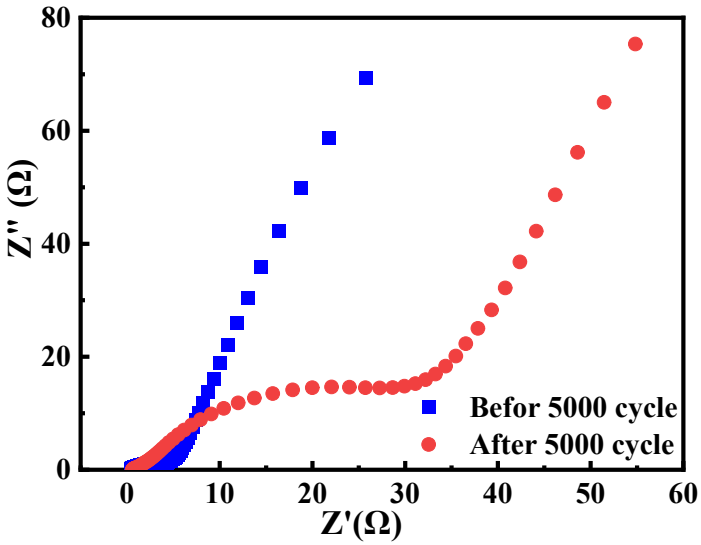

Fig. S10. Nyquist plots of CDP-MX/PA||CDP-MX/PA device.

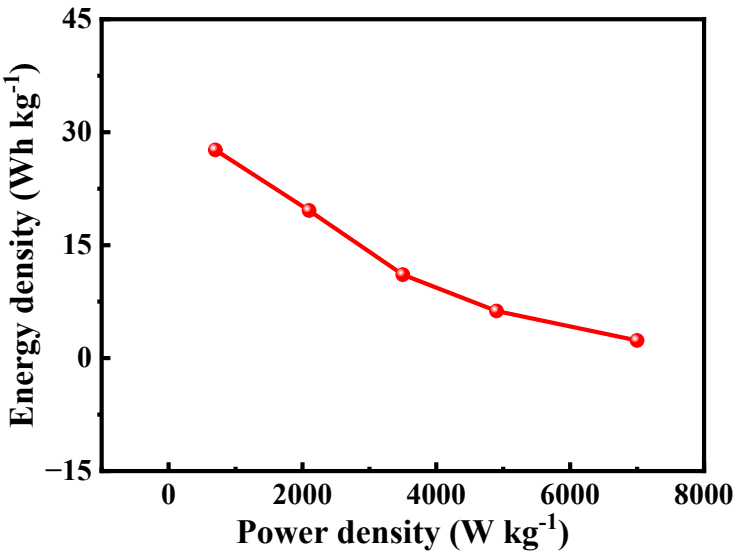

Fig. S11 Ragone plot of CDP-MX/PA||CDP-MX/PA device.